

*cy2*

# DUST PARTICLE VELOCITY MEASUREMENTS USING A LASER VELOCIMETER



V. A. Cline, Jr.

ARO, Inc.

December 1972

Approved for public release; distribution unlimited.

**ARNOLD ENGINEERING DEVELOPMENT CENTER  
AIR FORCE SYSTEMS COMMAND  
ARNOLD AIR FORCE STATION, TENNESSEE**

Property of U. S. Air Force  
AEDC LIBRARY  
#40500-73-C-0004

# ***NOTICES***

When U. S. Government drawings specifications, or other data are used for any purpose other than a definitely related Government procurement operation, the Government thereby incurs no responsibility nor any obligation whatsoever, and the fact that the Government may have formulated, furnished, or in any way supplied the said drawings, specifications, or other data, is not to be regarded by implication or otherwise, or in any manner licensing the holder or any other person or corporation, or conveying any rights or permission to manufacture, use, or sell any patented invention that may in any way be related thereto.

Qualified users may obtain copies of this report from the Defense Documentation Center.

References to named commercial products in this report are not to be considered in any sense as an endorsement of the product by the United States Air Force or the Government.

DUST PARTICLE VELOCITY MEASUREMENTS  
USING A LASER VELOCIMETER

V. A. Cline, Jr.  
ARO, Inc.

Approved for public release; distribution unlimited.

## FOREWORD

The work reported herein was conducted at the Arnold Engineering Development Center (AEDC), Air Force Systems Command (AFSC), Arnold Air Force Station, Tennessee, under Program Element 65802F.

The results of the research were obtained by ARO, Inc. (a subsidiary of Sverdrup & Parcel and Associates, Inc.), contract operator of AEDC under Contract F40600-73-C-0004. The research was conducted from November 1971 through February 1972 under ARO Project No. BF319, and the manuscript was submitted for publication on August 23, 1972.

The author wishes to acknowledge the assistance of F. H. Smith, Jr., Technical Staff, in the preparation of this report.

This technical report has been reviewed and is approved.

JOHN R. TAYLOR  
Major, USAF  
Research & Development Division  
Directorate of Technology

ROBERT O. DIETZ  
Acting Director  
Directorate of Technology

**ABSTRACT**

This report describes the use of a one-component dual-scatter laser velocimeter (LV), in the forward-scatter mode, to measure the particle velocity distribution in a hypersonic dust erosion facility. The data acquired from a number of experiments are briefly summarized. Additional data acquired from holographic and fiber-optics measurements are also compared with the LV data. A discussion of the effects of both periodic and nonperiodic electrical noise upon the data is presented.

## CONTENTS

	<u>Page</u>
ABSTRACT . . . . .	iii
I. INTRODUCTION . . . . .	1
II. LASER VELOCIMETER – DESCRIPTION . . . . .	1
III. DUST EROSION TUNNEL – DESCRIPTION . . . . .	3
IV. TEST PROCEDURES, RESULTS, AND DISCUSSION	
4.1 Holographic Data Comparisons . . . . .	4
4.2 Noise Problems . . . . .	5
4.3 Data Acquisition Rate . . . . .	5
V. SUMMARY OF RESULTS . . . . .	7
REFERENCES . . . . .	8

## APPENDIX ILLUSTRATIONS

### Figure

1. Dual-Scatter Optical Arrangement . . . . .	11
2. Interference Fringes in Beam Crossover Region . . . . .	12
3. LDV Collection Package . . . . .	13
4. Dust Erosion Tunnel . . . . .	14
5. Calculated Particle Velocities versus Particle Size . . . . .	15
6. Velocity versus Time of Acquisition – Run No. 8 . . . . .	16
7. Velocity Distribution – Run No. 8 . . . . .	17
8. Size Distribution of MgO Dust from PWT Dust Erosion Tunnel . . . . .	18
9. Velocity versus Time of Acquisition – Run No. 6 . . . . .	19
10. Velocity Distribution – Run No. 6 . . . . .	20
11. Velocity versus Time of Acquisition – Run No. 7 . . . . .	21
12. Velocity Distribution – Run No. 7 . . . . .	22
13. Velocity versus Time of Acquisition – Run No. 9 . . . . .	23
14. Velocity Distribution – Run No. 9 . . . . .	24

<u>Figure</u>	<u>Page</u>
15. Velocity versus Time of Acquisition – Run No. 16 . . . . .	25
16. Velocity Distribution – Run No. 16 . . . . .	26
17. Velocity versus Time of Acquisition – Run No. 12 . . . . .	27
18. Velocity Distribution – Run No. 12 . . . . .	28
19. Velocity Distribution Obtained by Holographic Technique – Run No. 1 . . . . .	29
20. Velocity Distribution Obtained by Three Experimental Techniques . . . . .	30
21. LV Probe Volume Illustration . . . . .	31

## SECTION I INTRODUCTION

The hypersonic Dust Erosion Tunnel (DET), Propulsion Wind Tunnel Facility (PWT), AEDC, is being used to study the effects of the high-energy impact of dust particles on various targets. A knowledge of the particle velocity on impact is imperative. The laser velocimeter (LV) has been proven ideal for measuring these velocities. The LV measures the shift in frequency of the laser radiation scattered from the moving particles. The data are, therefore, a direct measure of the velocity of the particles as opposed to an indirect determination using the gas velocity and drag laws.

The LV development at AEDC is well documented. (Refs. 1, 2, 3, 4, and 5.) The LV systems have been used in actual test situations during the development phase and have shown good results (Refs. 4 and 5). During the present work, the dual-scatter, off-axis collection configuration was used to perform the measurements.

## SECTION II LASER VELOCIMETER – DESCRIPTION

The dual-scatter LV system in the off-axis forward-scatter arrangement is shown in Fig. 1 (Appendix). The laser beam is split into two parallel beams, compensated for optical path length, through the self-aligning optics package (Ref. 2). The two beams are then focused to a common point by lens  $L_1$ . The angle of convergence ( $\theta$ ) of the beams is dependent on the beam separation obtained through the beam-splitting blocks and the focal length of  $L_1$ . At the focal point, interference of the two beams takes place to provide the fringe pattern, as described below. The detection system consists of a lens ( $L_2$ ) and a photomultiplier (PM) tube to collect the radiation scattered from within the focal volume to provide the alternating current for processing.

In the crossover region (focal region) the two beams consist of plane waves. Figure 2 represents this region with the lines normal to the beam axes illustrating adjacent wave crests of maximum intensity. The interference phenomenon produces a series of bright and dark fringes oriented in the x, y plane so that y is constant.

It is shown in Fig. 2b that the fringe spacing ( $\delta$ ) is  $\delta = \lambda / [2 \sin (\theta/2)]$ . As a particle traverses the fringe region, the period of the signal

obtained is the time required to travel one fringe space. Thus, the velocity component normal to the fringes is  $V_n = f\lambda / [2 \sin (\theta/2)]$ , where  $f$  is the signal frequency.

It is important to note that the signal frequency is independent of the viewing angle, which was not true in the earlier LV configurations. This leads to great flexibility in adapting this system to practical test applications. A detailed treatment of laser Doppler velocimeter (LDV) theory is found in Ref. 1, where the mathematical derivation of the Doppler effect obtains the same result as that shown above.

A measurement of one component of the velocity (along the tunnel centerline) is satisfactory for this application, although gross errors could result if the particle trajectory varied significantly from the selected component. In the present case, with a very long nozzle with angles of divergence of 2 deg, the measured velocity could vary less than 0.1 percent from the actual velocity because of trajectory error ( $V_m = V_a \cos 2 \text{ deg}$ ).

The input radiation source for the velocimeter was an argon laser with a nominal output of 0.10 w at 4880-Å wavelength in the transverse electromagnetic ( $TEM_{00}$ ) mode. The input optics consisted of the self-aligning beam-splitting blocks and a 6-in.-diam, 90-in. focal length focussing lens. A polarization rotator was used to optimize power and to balance the intensity of the two beams downstream of the beam-splitting blocks. The two beams each contained, generally, about 16 MW of power. The laser was operated in a semidonut mode (near  $TEM_{11}$ ), which gave a somewhat larger probe volume than a Gaussian mode and also increased the power output by about 100 percent. The beams were directed by two plane, front-surface mirrors into the test cell, with the focal point on the test cell centerline.

The collection package (Fig. 3) contained two 6-in.-diam lenses with 30- and 49-in. focal lengths back to back, which imaged a conical portion of the beam crossover region onto a pin hole (0.040-in. diameter) located immediately in front of the PM tube.

The alignment of the collection optics is very critical. Alignment was accomplished by placing a scattering source in the probe volume center and aligning the PM tube and pin hole with a precision x, y, z micropositioner. The alternating scattered signal from the PM tube is amplified and fed to the Doppler Data Processor\* (DDP)(Ref. 1), which

---

\*Patent Pending.

checks the signal for periodicity for a given number of cycles and then determines its period. (If the signal is not periodic within 2 percent, it is rejected.) The period is then recorded both on a paper tape printer and on magnetic tape for computer interfacing. A millisecond clock is incorporated in the recording system so that the time each data point was acquired is also printed.

The computer calculates the velocity and plots out both the velocity distribution, including all data points of a given run, and a plot of velocity versus time of data acquisition. The clock is started by a relay connected to the test facility arc starting unit so that the data acquisition time is correlated with PWT data.

### SECTION III DUST EROSION TUNNEL – DESCRIPTION

The AEDC Dust Erosion Tunnel is a continuous-flow, arc-heated wind tunnel in which erosion tests of materials under high-velocity, high-enthalpy conditions can be conducted. A schematic of the facility is shown in Fig. 4.

Magnesium oxide (MgO) dust particles are injected upstream of the hypersonic nozzle throat and are aerodynamically accelerated. The velocity versus particle size is shown in Fig. 5 for normal tunnel conditions. The basic aerodynamic drag equation, with the assumption that the particles are spherical in shape, was used in calculating the values presented (see Ref. 6). A multiple-mount model-positioning system is enclosed in the test cell for model injection into the flow.

### SECTION IV TEST PROCEDURES, RESULTS, AND DISCUSSION

The test activity varied with each run conducted in the tunnel. After a nominal 40 to 60 sec required for arc stabilization, from one to six models were sequentially injected into the test flow. After a time in dust-free flow the MgO particles, of nominal 100- $\mu$ m diameter, were introduced for a specified length of time (usually from 5 to 20 sec). The data processor was started at the time of arc ignition. The time history of run number 8 is shown in Fig. 6, where each data point was plotted versus time of acquisition.

The dust-free periods between model injections are clearly seen. The data from all the dust periods during run number 8 are shown combined in Fig. 7. The most frequently obtained velocity was 5600 ft/sec. The spread in velocities shown was mainly caused by the spread in diameter of the dust particles about the mean diameter of 100  $\mu\text{m}$ . This fact was established from the holographic studies carried on concurrently in the DET. A laboratory determination of the size distribution was also made, using a fiber-optics array method currently under study at AEDC (Ref. 7). The size distribution using this technique is shown in Fig. 8. The theoretical considerations in Fig. 5 indicate that this dust size distribution should produce velocities ranging from 3400 ft/sec up to approximately 9500 ft/sec. Thus, it is seen that the LV distributions obtained will depend primarily on the particle size distribution although there is surely a range of velocities for each discrete size. Typical data are shown in Figs. 9 through 18.

#### 4.1 HOLOGRAPHIC DATA COMPARISON

A newly developed, double-pulse holography system was used to obtain velocity data on a different, but equivalent, run in the DET. This system makes a hologram of a portion of the test section at two instants of time separated by about 1 msec (see Ref. 8). This technique allows a time-distance determination of velocity of the individual particles in the hologram. In addition, the size of these particular particles can be determined. One disadvantage of holography is that the data are valid only for one instant of time (1 msec) during the dust period. As shown by the LV data in Fig. 6, the velocity distribution seems to vary with time as might be expected. For instance, the range of velocities at 68 sec is much less than that at 118 sec. The results of a holographic analysis are presented in Fig. 19. It shows approximately the same range of velocities as the LV results, with the distribution peaks occurring at nearly the same velocities. The LV distribution in Fig. 10 compares exceedingly well in shape and range with the holographic data.

All of the LV data from runs of equivalent tunnel conditions were compiled into one total velocity distribution. These data are shown in Fig. 20 superimposed on the data from the two other experimental techniques discussed, the holographic data (one run only) and the fiber-optics sizing technique. The fiber-optics size distribution was converted into a velocity distribution using the data in Fig. 5. The velocity peaks fall within 500 ft/sec of each other (9.1-percent deviation from LV peak) with the holographic and LV data showing only a 200-ft/sec difference (4.6 percent). Based on microscopic examination of the dust particles, the dashed line extrapolated from the fiber-optics curve is felt to be a reasonable approximation of the trend of the data.

## 4.2 NOISE PROBLEMS

The noise level in the systems varied considerably from day to day, presumably because of the other test activities in the area of the DET. One definite noise source was traced to arc noise introduced in a cable from the LV equipment to the control room. This source was removed, but an intermittent noise problem persisted throughout the tests. Figure 17 shows the results of what appears to be a high-frequency noise band at 4600 ft/sec. This noise is evident because it appears during periods of nondusting, especially during the first 40 sec of arc stabilization. Attempts to isolate the problems were frustrated by the fact that the tunnel run time was seldom more than 2 to 3 min and occurred no more than once a day.

Fortunately, when a noise band exists in the data, it is evident on the velocity-time plot, and valid data can still be extracted. Clean breaks between dust periods assure that the data are unaffected by noise.

The threshold level at which the signal will trigger the processor and be recorded is variable. Since each run seemed to have a different associated noise level, the trigger level had to be adjusted accordingly during the first of each run. Also, since the high-velocity end of the range would come from signals from the smaller particles, and therefore the lower signal levels, it is important to detect the smallest possible signals. The process of setting the trigger so that it is above noise level, but still getting the small amplitude signals, is very critical. The procedure used was to set the trigger level manually so that the noise would trigger the system and then to increase the threshold just above this level. This was done while the arc conditions were being set, and no dust was introduced. A better procedure would require a continuously-variable-gain amplifier instead of the step-gain amplifier used. Then the existing noise could be amplified to just below the minimum processor threshold of 20 MV. This would optimize the collection of high-frequency signals.

## 4.3 DATA ACQUISITION RATE

The average rate of particle mass flow was found for each run by weighing the sample in the "hopper" before and after the run. A typical value for what was considered heavy dusting was (for run number 9)  $68.8 \times 10^{-8}$  gm/cm<sup>3</sup>. Assuming that the particles are spherical with 90- $\mu$ m diameter and a specific gravity of 3.58, the particle mass is seen to be  $1.37 \times 10^{-6}$  gm/particle. The particle concentration ( $N_p$ ) was then 0.5 particles per cubic centimeter of air.

For an estimate of the rate of particle flow through the probe volume, the cross-sectional sensing area normal to the flow is required. The actual probe volume is a very complicated intersection of two cylinders of different diameters and varying angles of intersection, all of which change from one LV application to the next. The volume is also a function of the electronic characteristics of the data processor in that a certain minimum number of cycles of the signal is required for processing. This sensitive area is estimated by use of the equations and sketches in Fig. 21. The height of this area is the portion of the crossed beams over which a particle can pass and cross a minimum of 10 fringes. (This particular processor required 10 cycles.) The width of the area is more difficult to obtain. Maximum width would be defined by the point marked  $10\delta$  in part (c) of Fig. 21, but this would only be for a particle passing directly through the center as shown in part (d). As the particle moves above or below the centerline toward the edge of the beam, the effective width decreases until the point along Z is reached where the centerline length of coincidence of the two cylinders is about  $15\delta$ . At this point any particle passing through within the height limitation (h) will see 10 fringes. For this estimate the average width is assumed to be where the centerline length of  $12\delta$  is reached.

As previously stated, the laser was operated in a semidonut mode, which is considerably larger in diameter than the Gaussian mode; therefore, since all the theory has been developed for Gaussian mode, the diameter (D) of the crossed beams was determined experimentally. The crossover point was magnified and projected onto a screen, where the fringes were visually counted. [The fringe spacing ( $\delta$ ) depends only on the wavelength ( $\lambda$ ) and the beam angle ( $\theta$ )]. In this configuration there were 18 fringes of  $8.02 \times 10^{-3}$  cm spacing each or a beam diameter of 1.44 mm.

By the use of the equations in Fig. 21, the sensitive area was estimated to be  $3 \times 10^{-2}$  cm<sup>2</sup>. Taking the theoretical gas velocity of about 9000 ft/sec, one can see that the probe region samples the gas at a rate of  $8.3 \times 10^3$  cm<sup>3</sup>/sec. With  $N_p = 0.5$  cm<sup>-3</sup>, this is an available data rate of about 4000 sec<sup>-1</sup>. The lowest dust density run thus far would be, using the above assumption, about 600 sec<sup>-1</sup>.

This rate is much greater than the capability of the system in its present configuration. Because of the requirement to record the time of each data point, the maximum data rate is 10 points/sec. On each run the data show that there were periods during which the maximum rate was reached, but in general the data were recorded at about 60 percent of maximum, or 6 points/sec. Since this is a very small percentage

of what was available, possible data rejection mechanisms were present, such as multiple particles simultaneously in the probe volume. Any mechanism which destroys the periodicity of the signal will cause rejection of that signal within the processor.

If one continues the logic of Fig. 21 and uses the shaded area of part (b) as the cross-sectional area of the probe volume, an estimate of the probe volume of about  $4 \times 10^{-3} \text{ cm}^3$  is obtained. However,  $N_p = 0.5 \text{ cm}^{-3}$ , i. e., there are only two particles per 1000 probe volumes sampled. The logical conclusion is that the signal rejection is being accomplished by random noise pulses. This noise is not periodic and, therefore, does not contribute erroneous data as did the high-frequency noise discussed above, but would prevent the system from obtaining all the available data. This is another reason that the threshold voltage for the processor must be optimized according to locally existing noise levels.

## SECTION V SUMMARY OF RESULTS

The dual-scatter LV system proved capable of measuring the hypersonic velocities produced in the dust erosion facility. Velocities greater than 8000 ft/sec were recorded. It was pointed out that the distribution in measured velocities was primarily due to the distribution in particle size; therefore, a determination of the accuracy of the system for this application was not made. The systematic error of the LV is felt to be no greater than 3 percent, primarily because of the frequency window width set within the data processor. On the one comparison with data from the very straightforward holographic technique, the velocity distribution peaks compared within 4.6 percent. The capability of recording the time of each data point was very useful in providing a time history of individual runs. The only significant operational problem encountered was the high-frequency electronic noise, which was easily detectable, and its effects were readily removed from the data. Greater emphasis will be placed on the setting of the threshold level for signal processing. The threshold must be low enough to insure acceptance of the low-amplitude, high-frequency pulses, yet high enough to prevent rejection of valid data by spurious noise pulses reaching the processor.

## REFERENCES

1. Lennert, A. E., Brayton, D. B., Crosswy, F. L., et al. "Summary Report of the Development of a Laser Velocimeter to be Used in AEDC Wind Tunnels." AEDC-TR-70-101 (AD871321), July 1970.
2. Brayton, D. B. "A Simple Laser Doppler Shift Velocimeter with Self-Aligning Optics." Proceedings of the Electro-Optical Systems Design Conference, September 16-18, 1969. New York, New York.
3. Brayton D. B. and Goethert, W. H. "A New Dual-Scatter Laser Doppler Shift Velocity Measuring Technique." Proceedings of the Sixteenth International ISA Aerospace Instrumentation Symposium, May 11-13, 1970.
4. Smith, F. H., Lennert, A. E., and Hornkohl, J. O. "Velocity Measurements in Aerodynamic Wind Tunnel (1T) Using a Laser Doppler Velocimeter." AEDC-TR-71-165 (AD737097), February 1972.
5. Goethert, W. H., Kalb, H. T., and Lennert, A. E. "Backscatter Laser Doppler Velocimeter Applied to PWT, 1T Wind Tunnel." AEDC-TR to be published.
6. Lewis, H. F. "Methods for the Performance Estimation and Design of Nozzles Used to Provide Dusty, Hypersonic Flow Environments." AEDC-TR-71-255 (AD890102L), December 1971.
7. Bentley, H. T. "Fiber-Optics Particle Sizing Systems." AEDC-TR to be published.
8. Trolinger, J. D. and Belz, R. A. "In-Line Holography in Dust Erosion Facilities, AEDC-TR to be published.

**APPENDIX  
ILLUSTRATIONS**

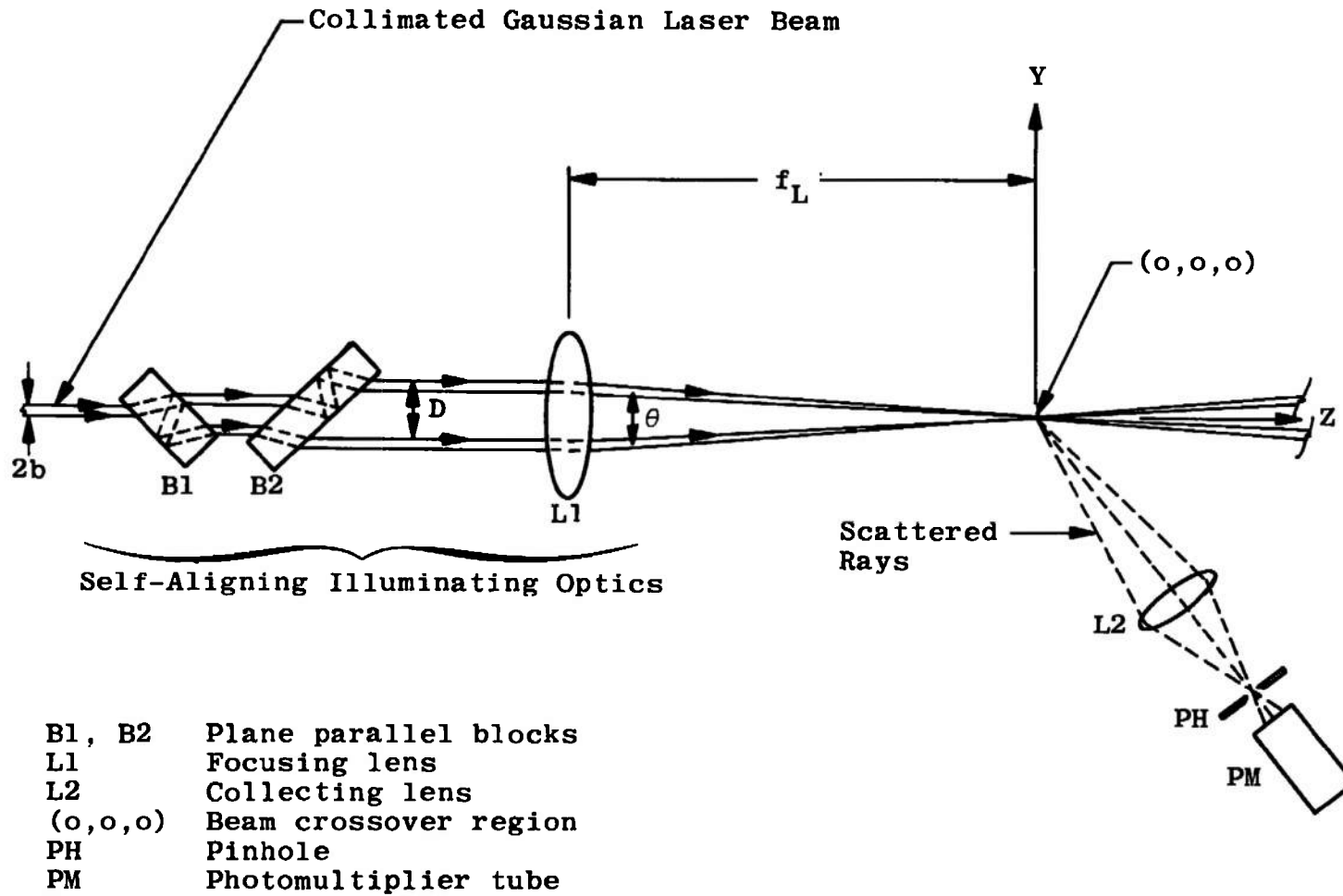
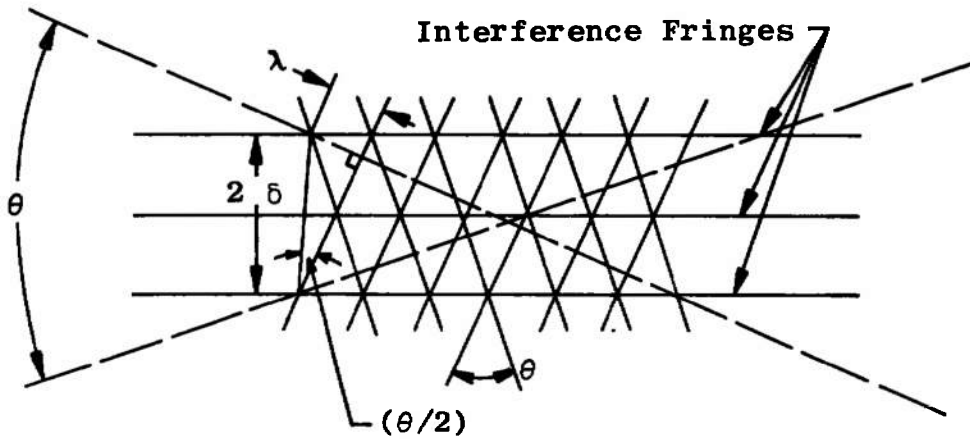
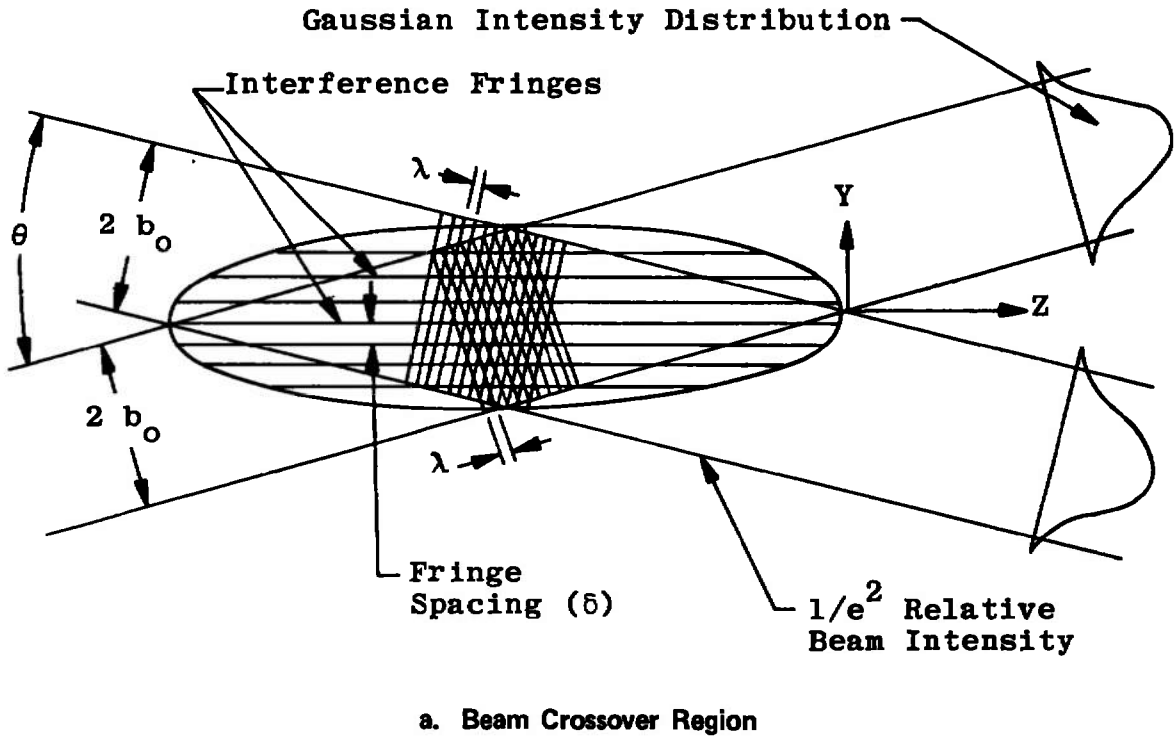


Fig. 1 Dual-Scatter Optical Arrangement



$$\sin \theta/2 = \frac{\lambda}{2\delta}$$

$$\text{Fringe Spacing } \delta = \frac{\lambda}{2 \sin (\theta/2)}$$

**b. Enlargement of Interference Region**  
**Fig. 2 Interference Fringes in Beam Crossover Region**

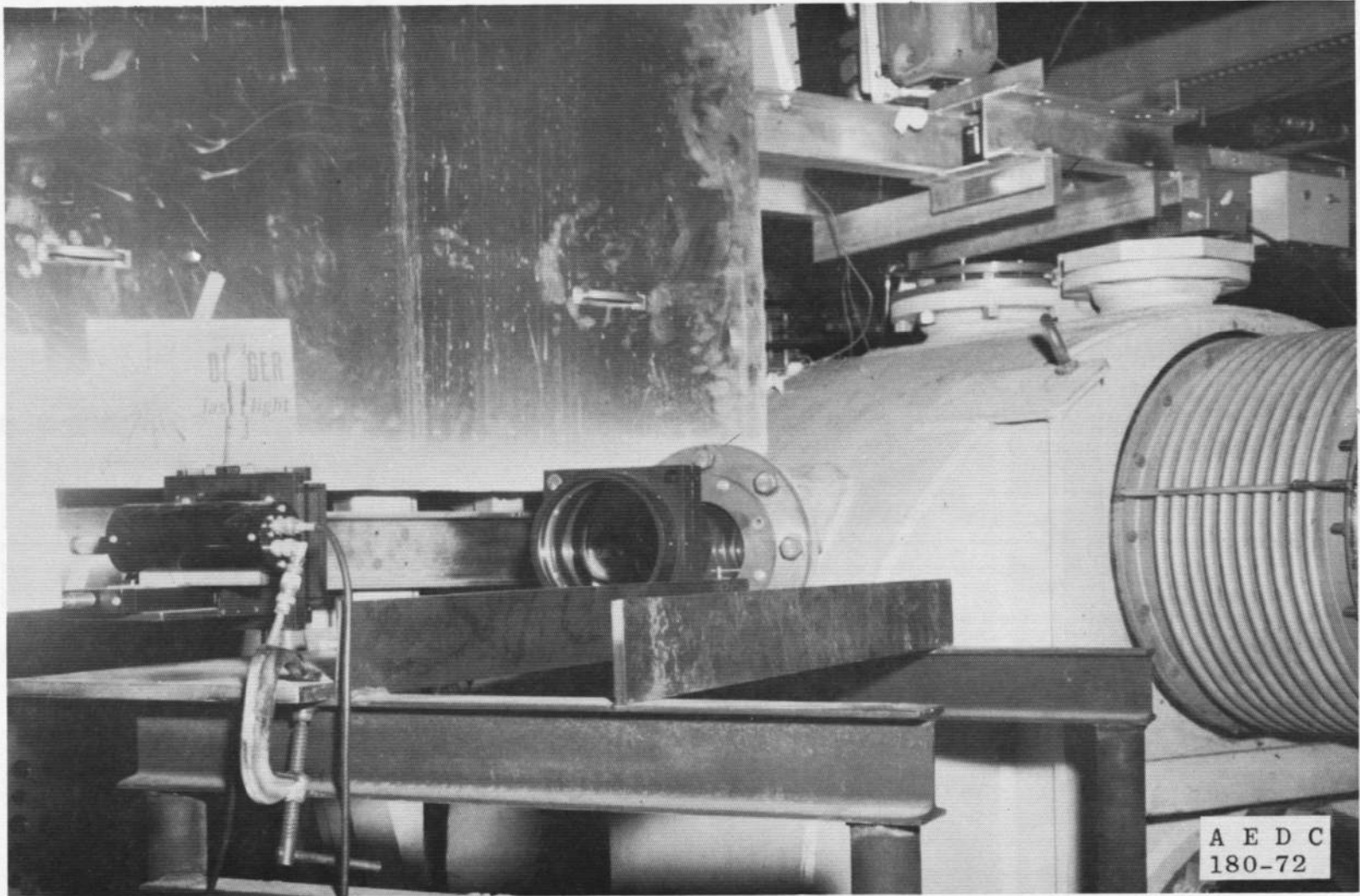


Fig. 3 LDV Collection Package

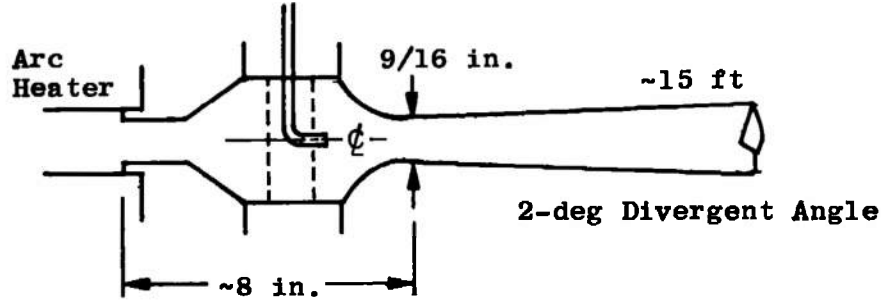
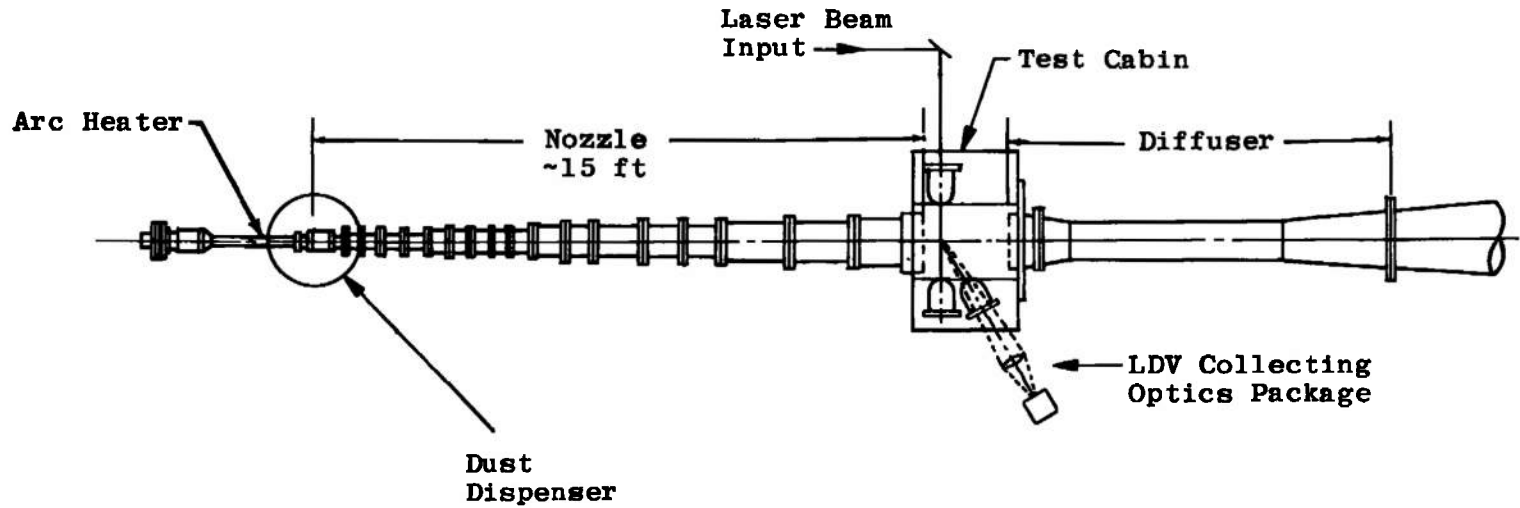
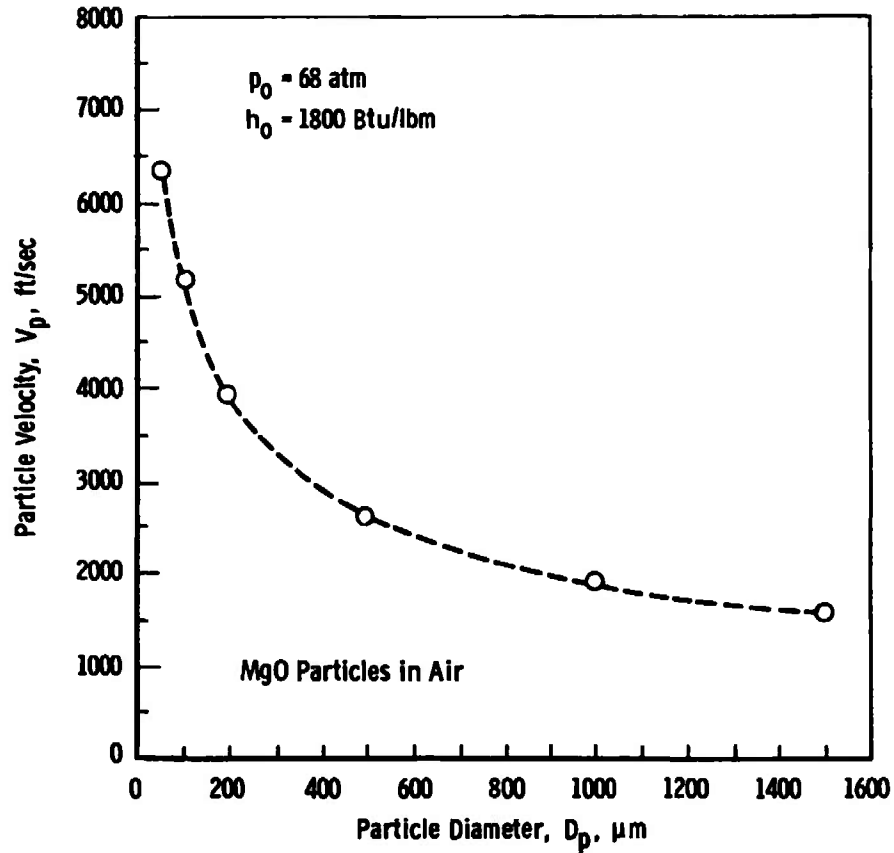
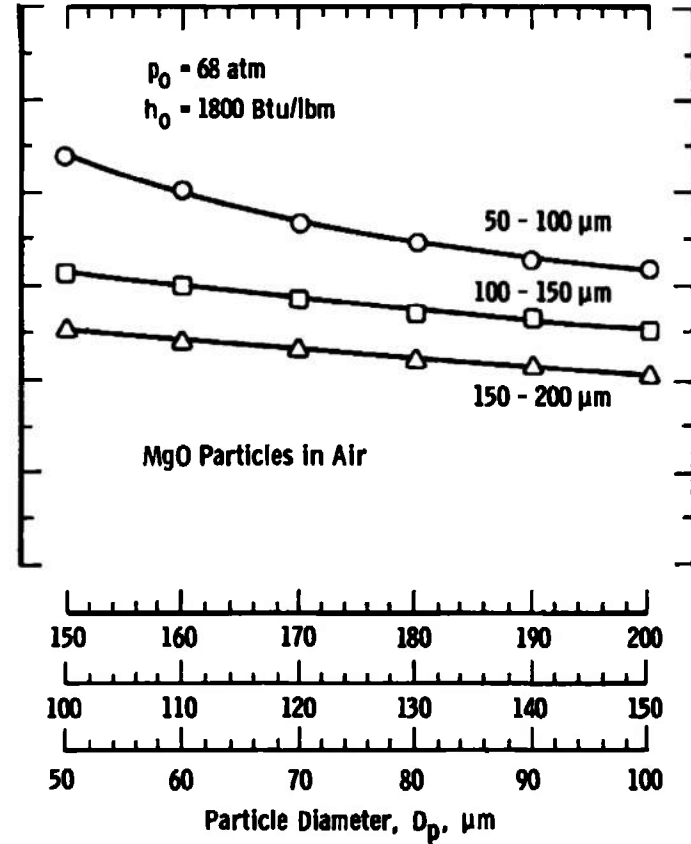


Fig. 4 Dust Erosion Tunnel



a. Comparison of the Differences in Particle Velocities Between Design and Operating Conditions



b. Expanded Size Scale for Operating Condition Particle Velocities

Fig. 5 Calculated Particle Velocities versus Particle Size

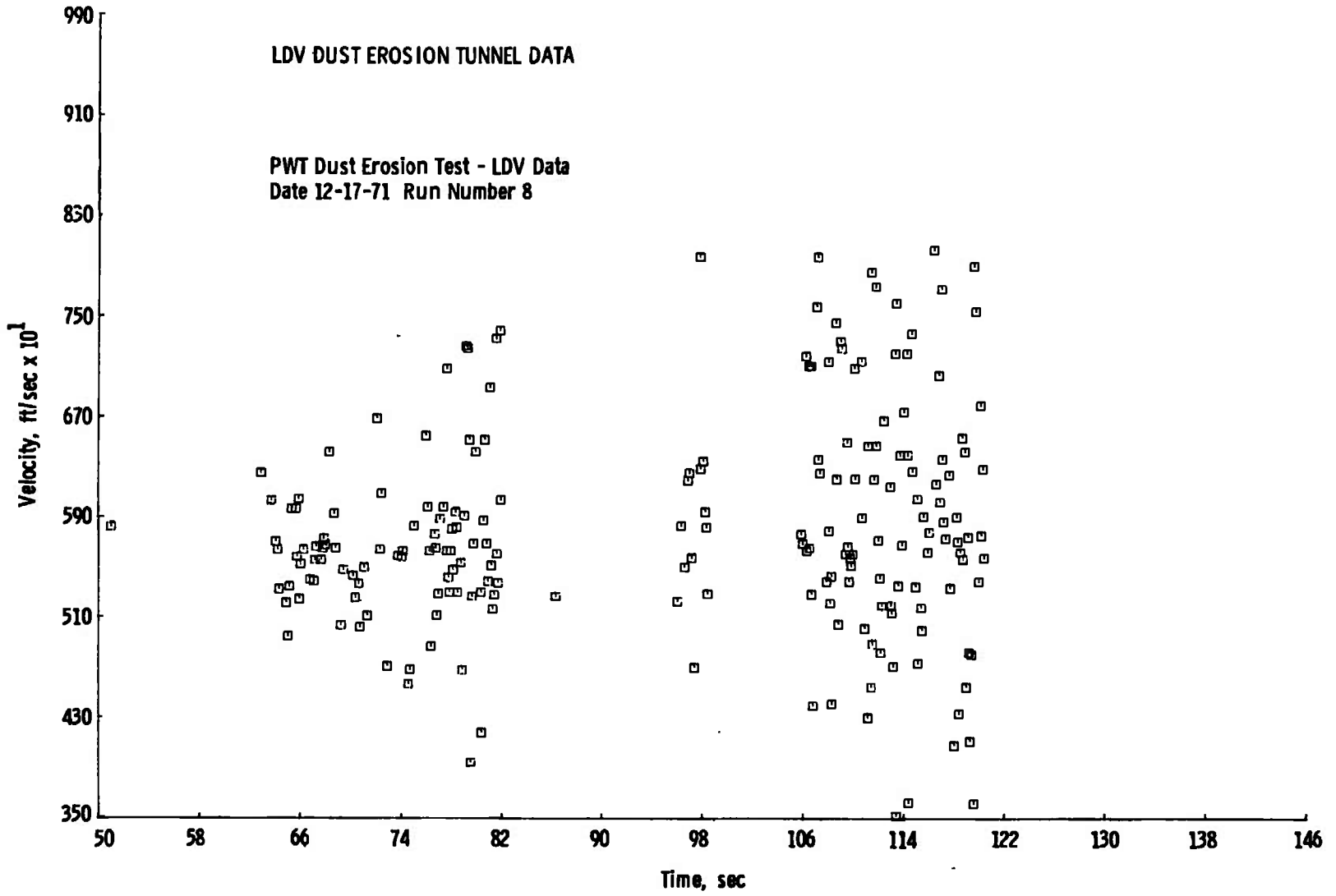


**Fig. 6 Velocity versus Time of Acquisition - Run No. 8**

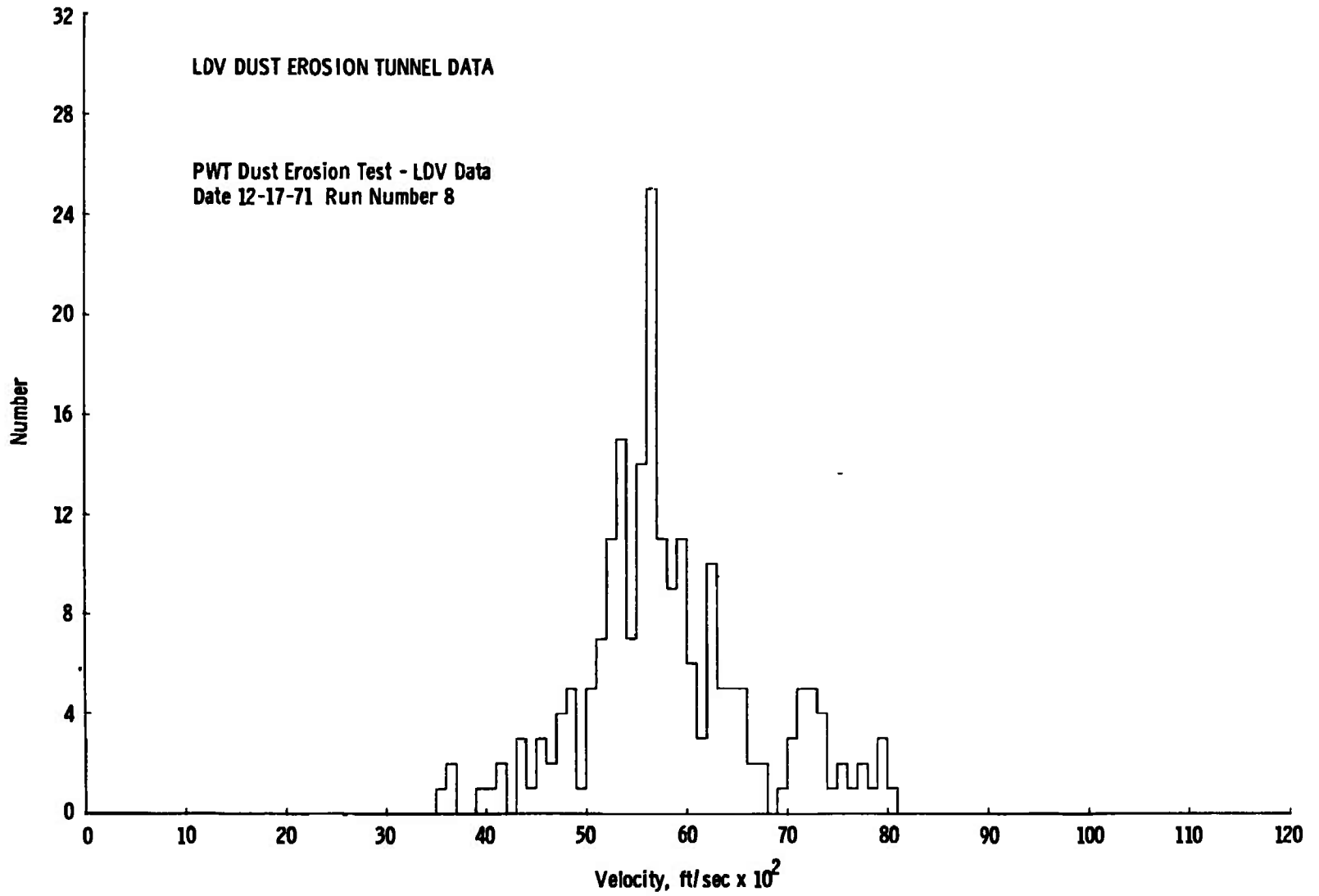


Fig. 7 Velocity Distribution - Run No. 8

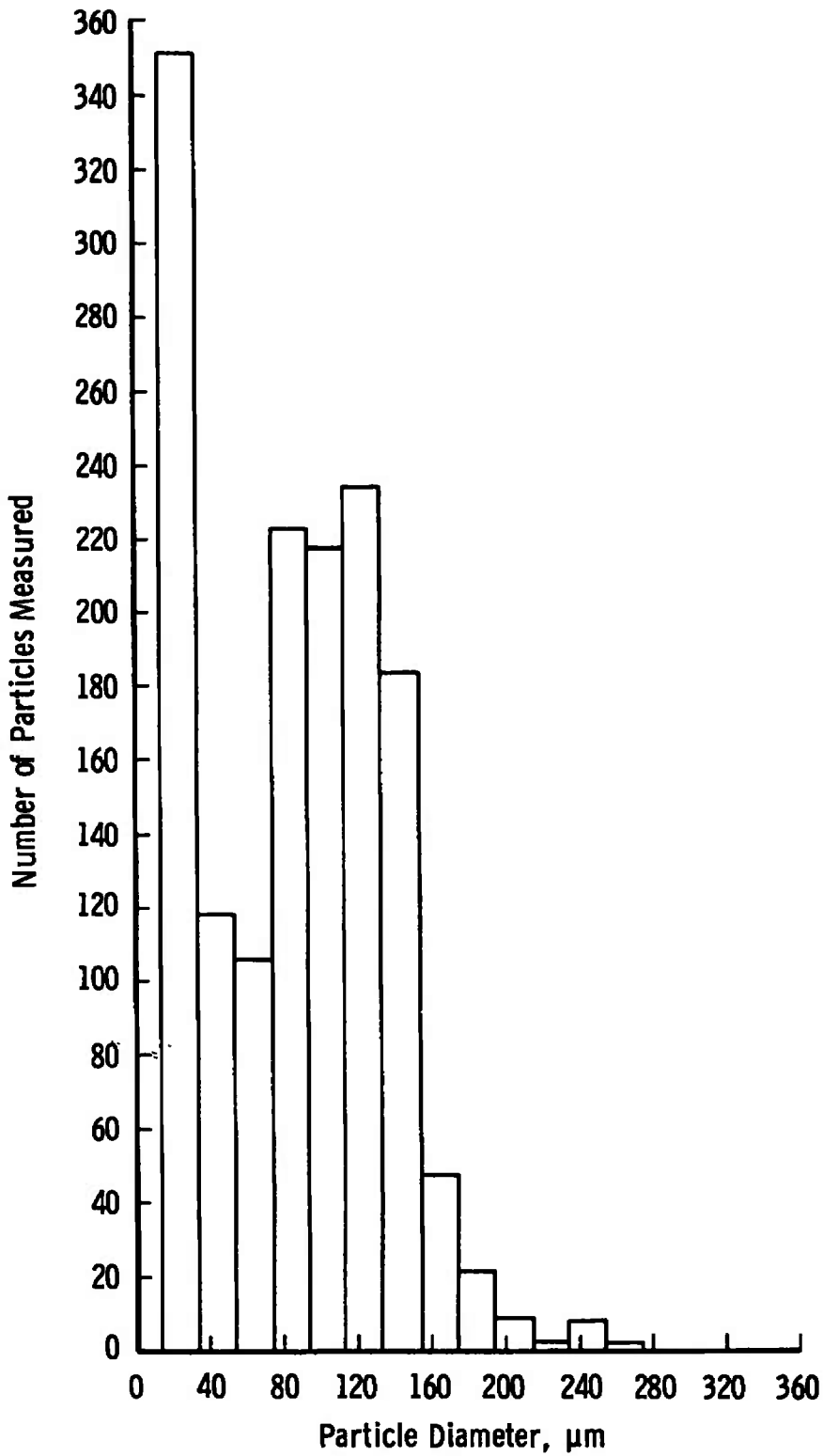


Fig. 8 Size Distribution of MgO Dust from PWT Dust Erosion Tunnel

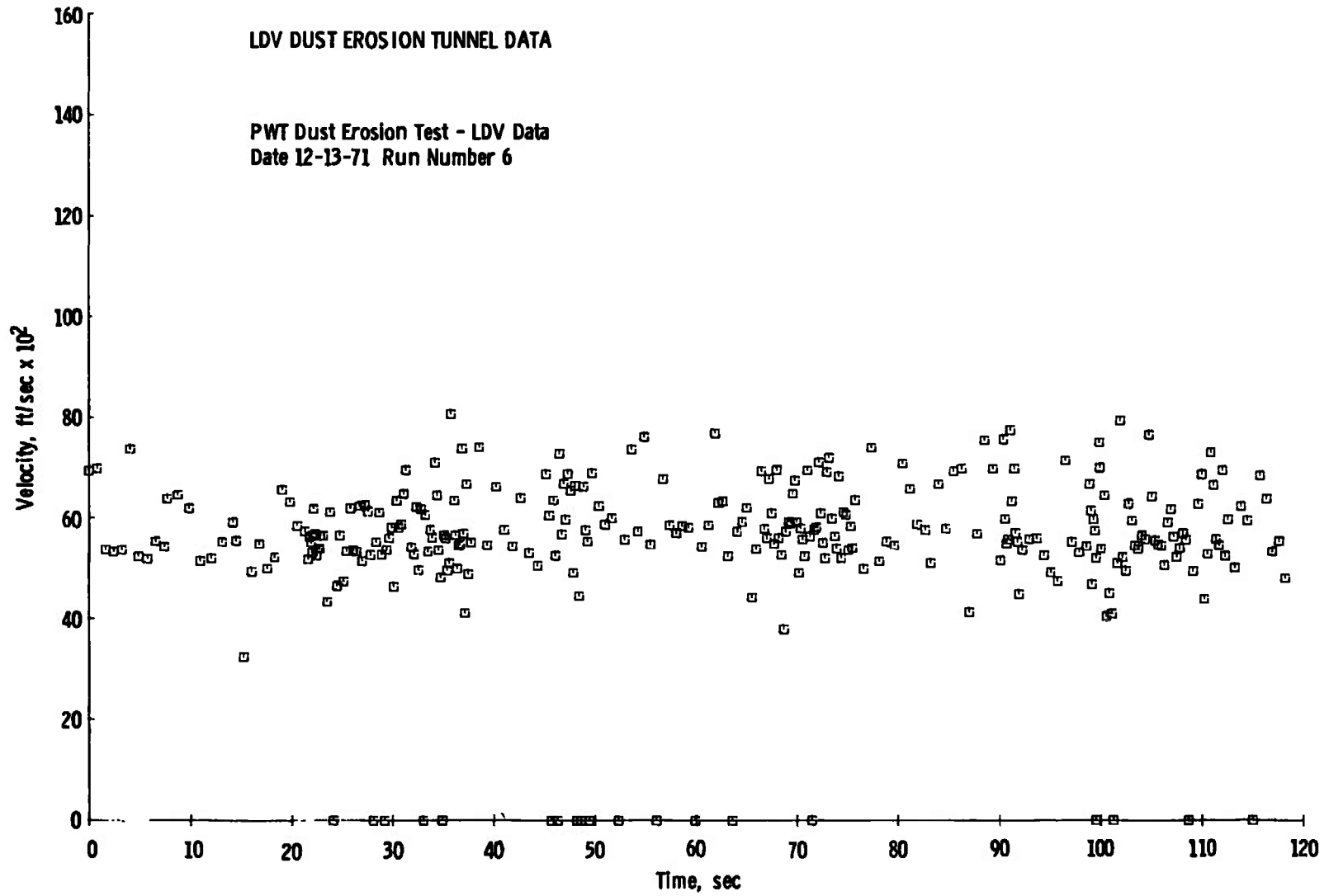


Fig. 9 Velocity versus Time of Acquisition – Run No. 6

LDV DUST EROSION TUNNEL DATA

PWT Dust Erosion Test - LDV Data  
Date 12-13-71 Run Number 6

20

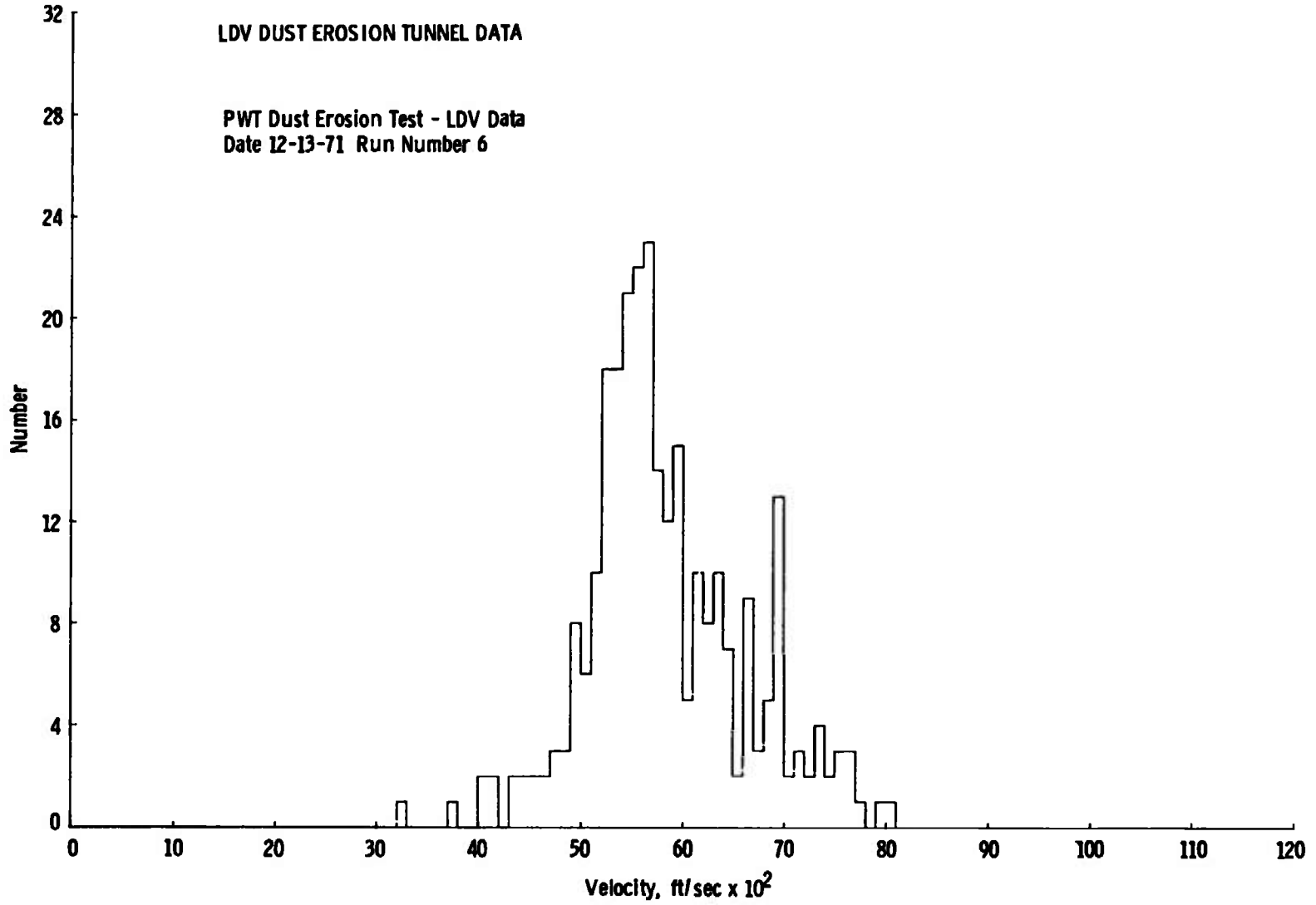


Fig. 10 Velocity Distribution - Run No. 6

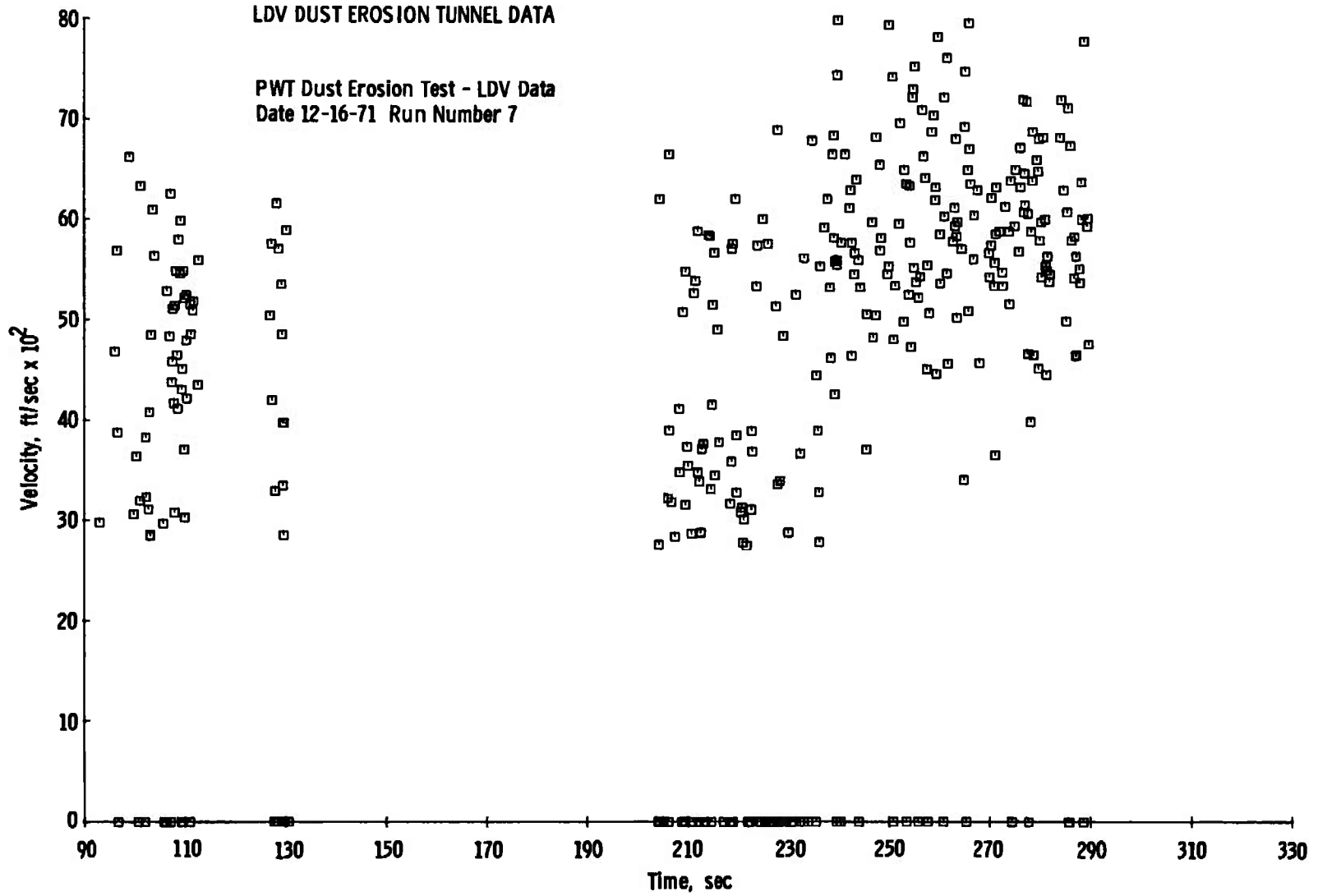
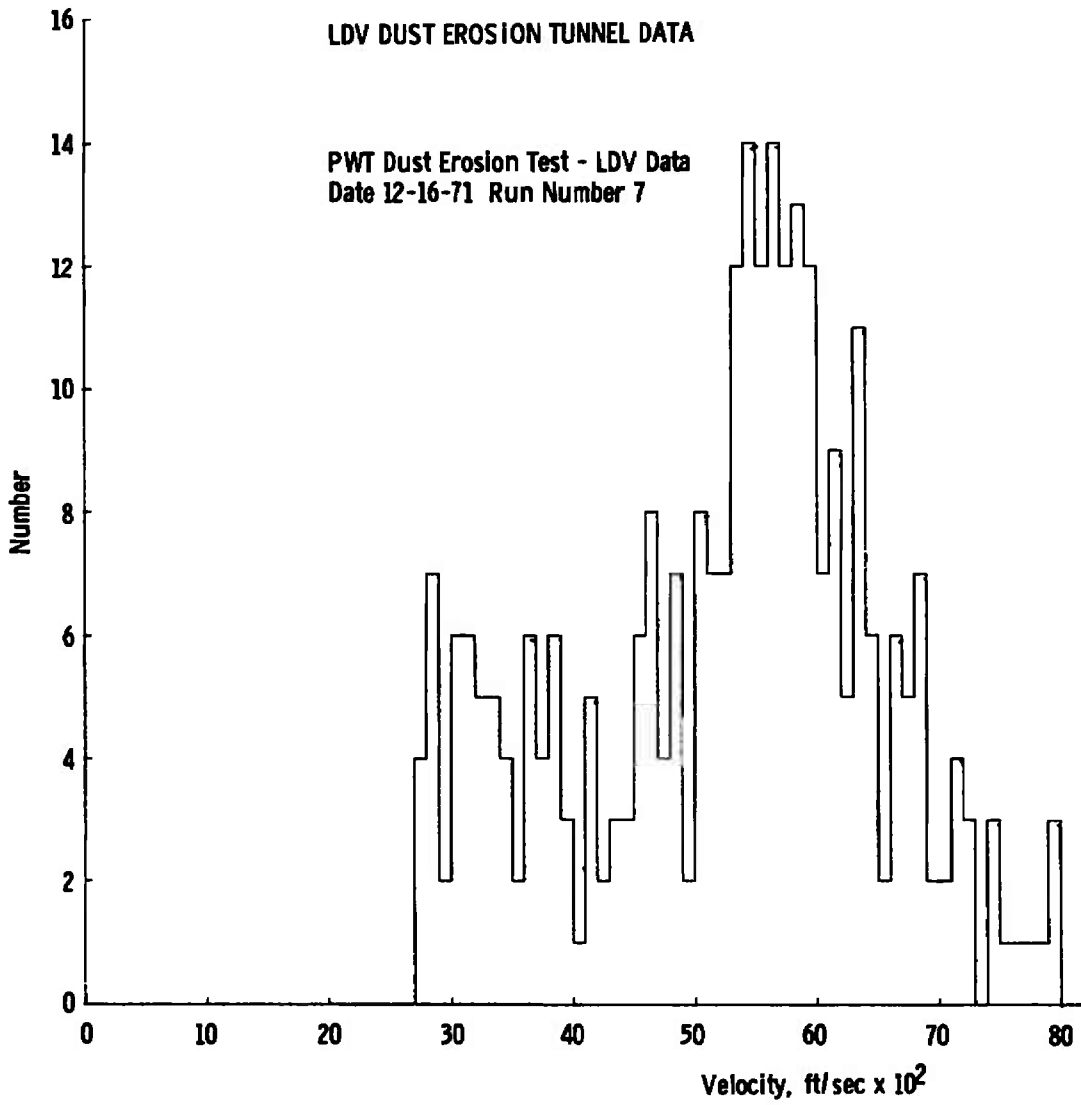


Fig. 11 Velocity versus Time of Acquisition - Run No. 7



**Fig. 12 Velocity Distribution – Run No. 7**

## LDV DUST EROSION TUNNEL DATA

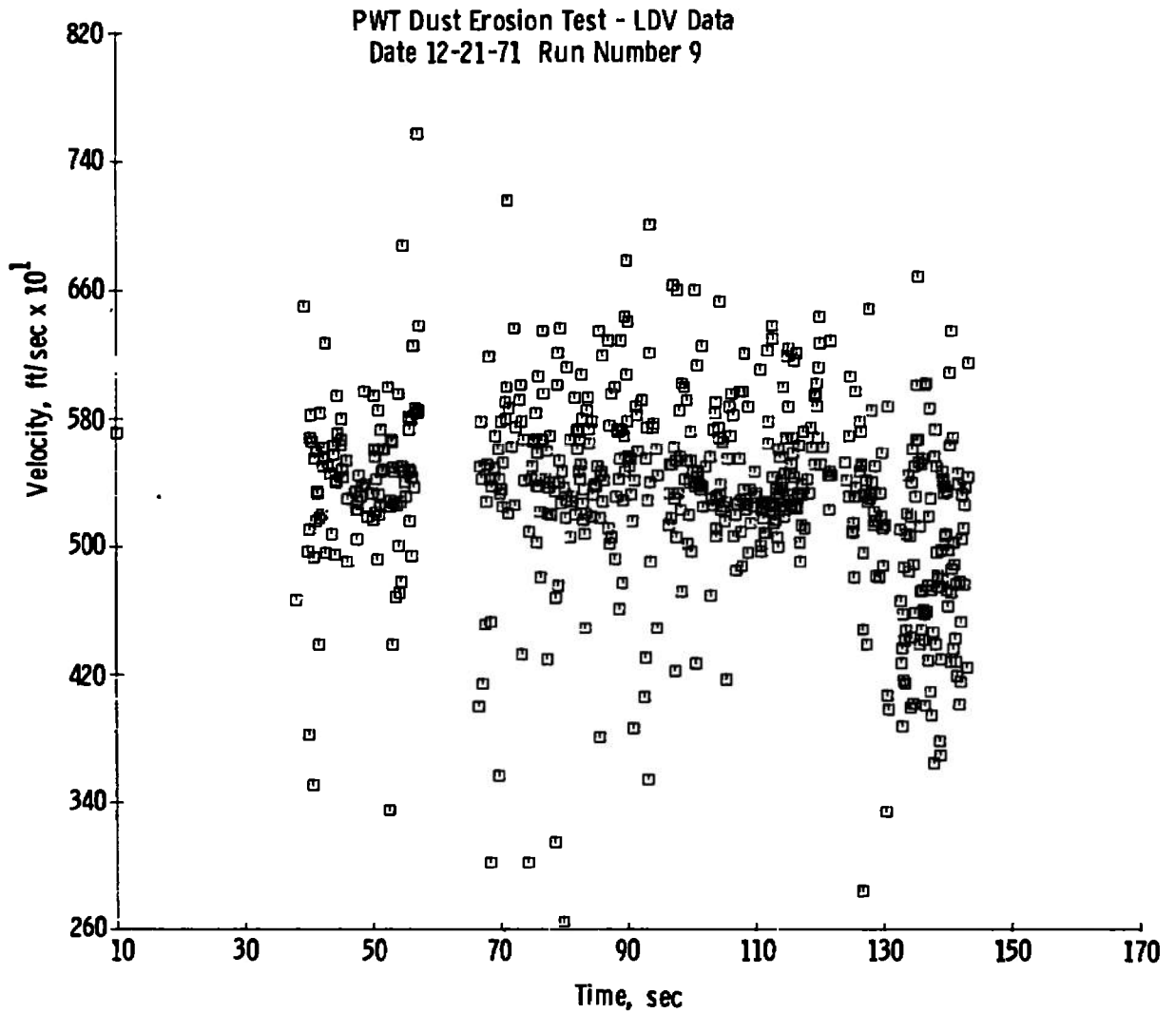


Fig. 13 Velocity versus Time of Acquisition — Run No. 9

LDV VELOCITY DISTRIBUTION DATA FROM DUST EROSION TUNNEL

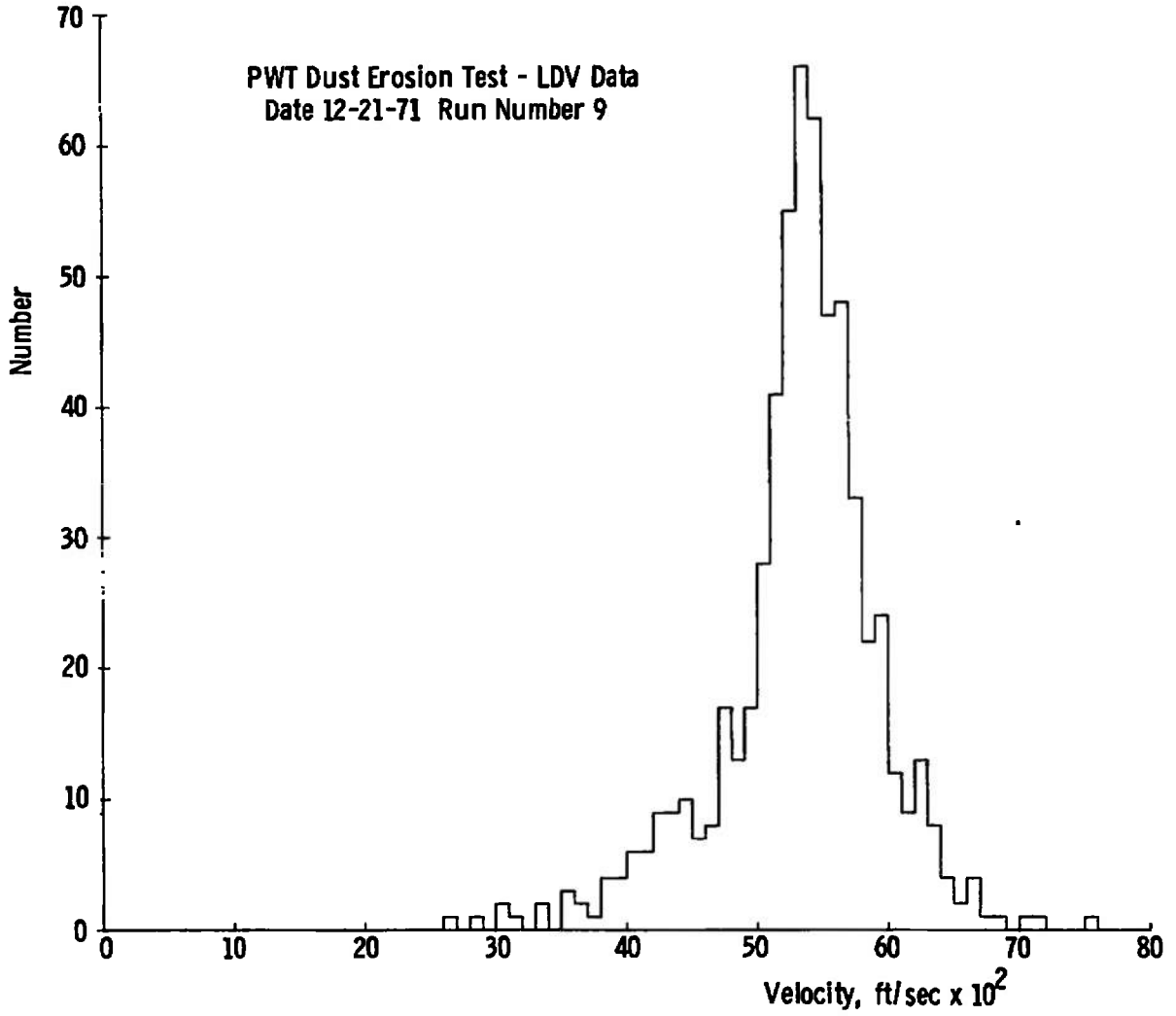


Fig. 14 Velocity Distribution — Run No. 9

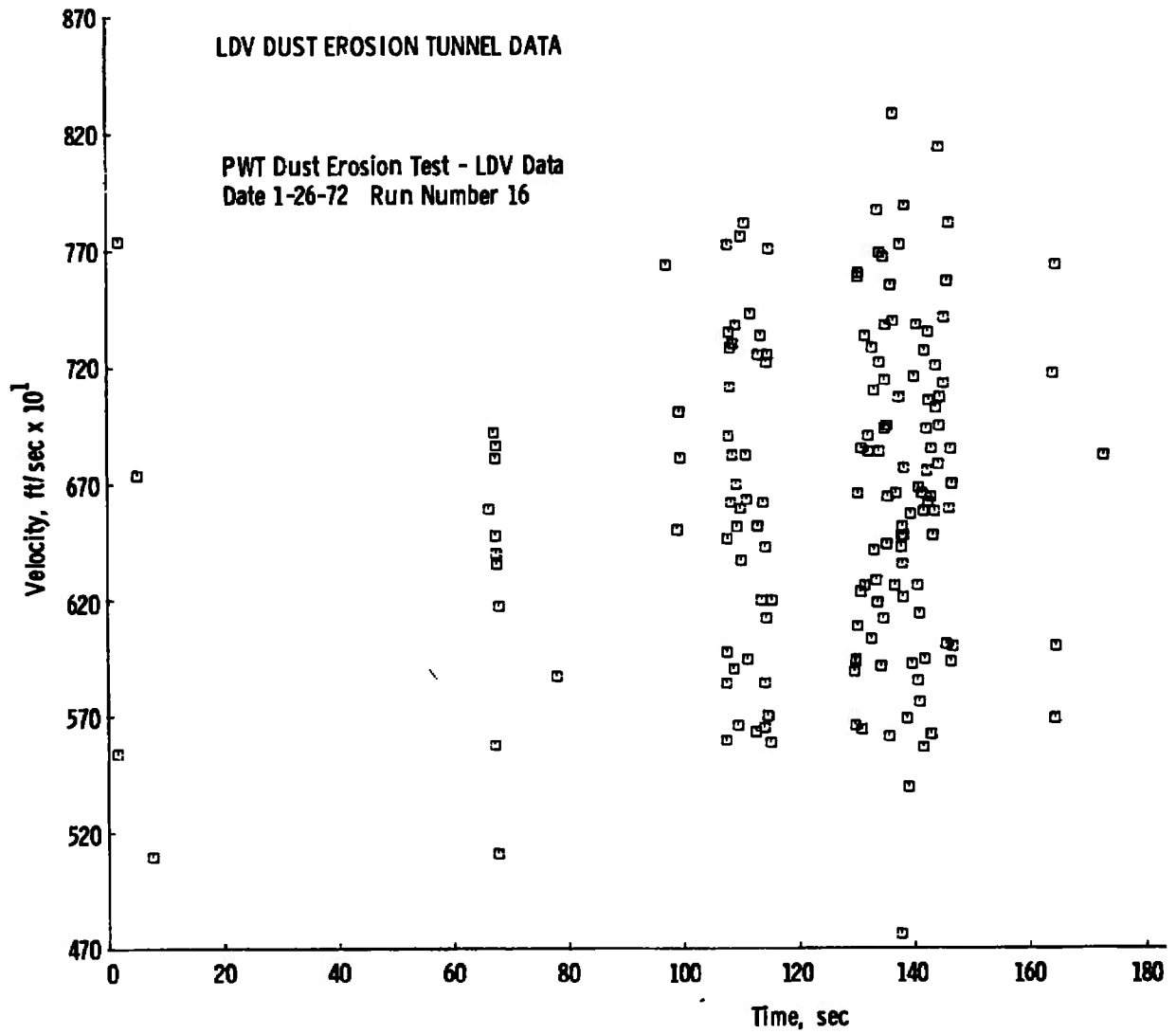


Fig. 15 Velocity versus Time of Acquisition — Run No. 16

LDV DUST EROSION TUNNEL DATA

PWT Dust Erosion Test - LDV Data  
Date 1-26-72 Run Number 16

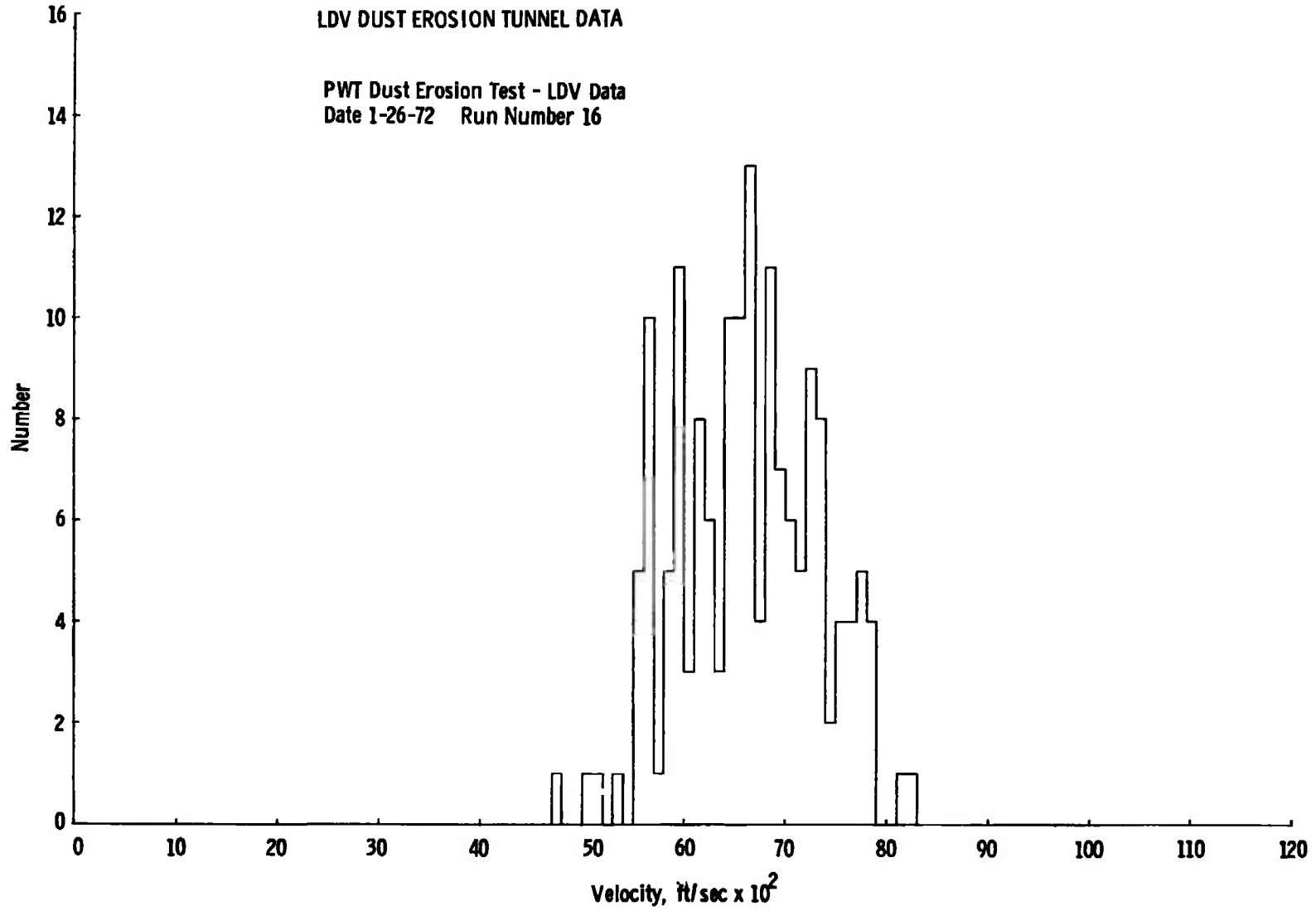
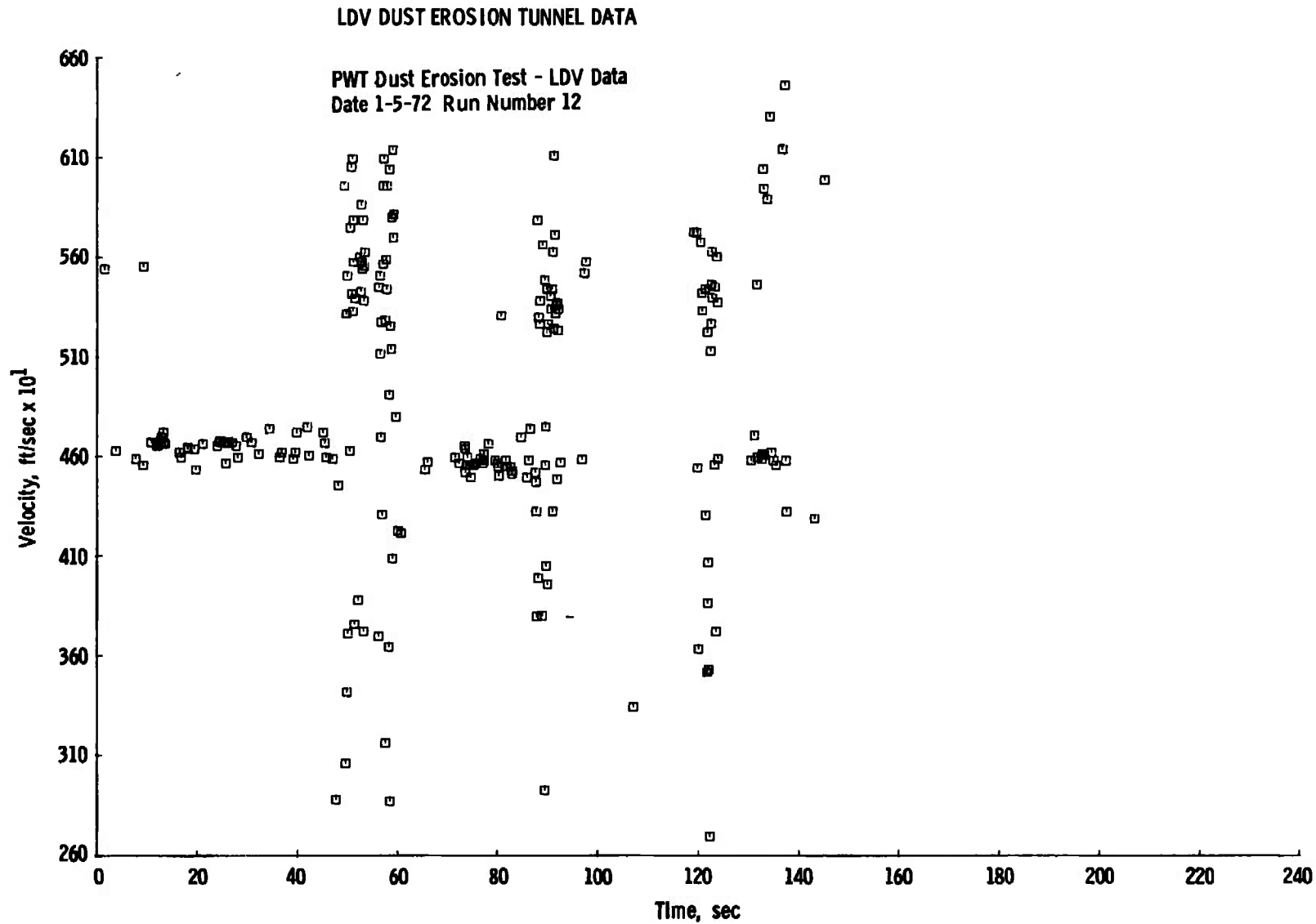


Fig. 16 Velocity Distribution — Run No. 16



**Fig. 17 Velocity versus Time of Acquisition – Run No. 12**

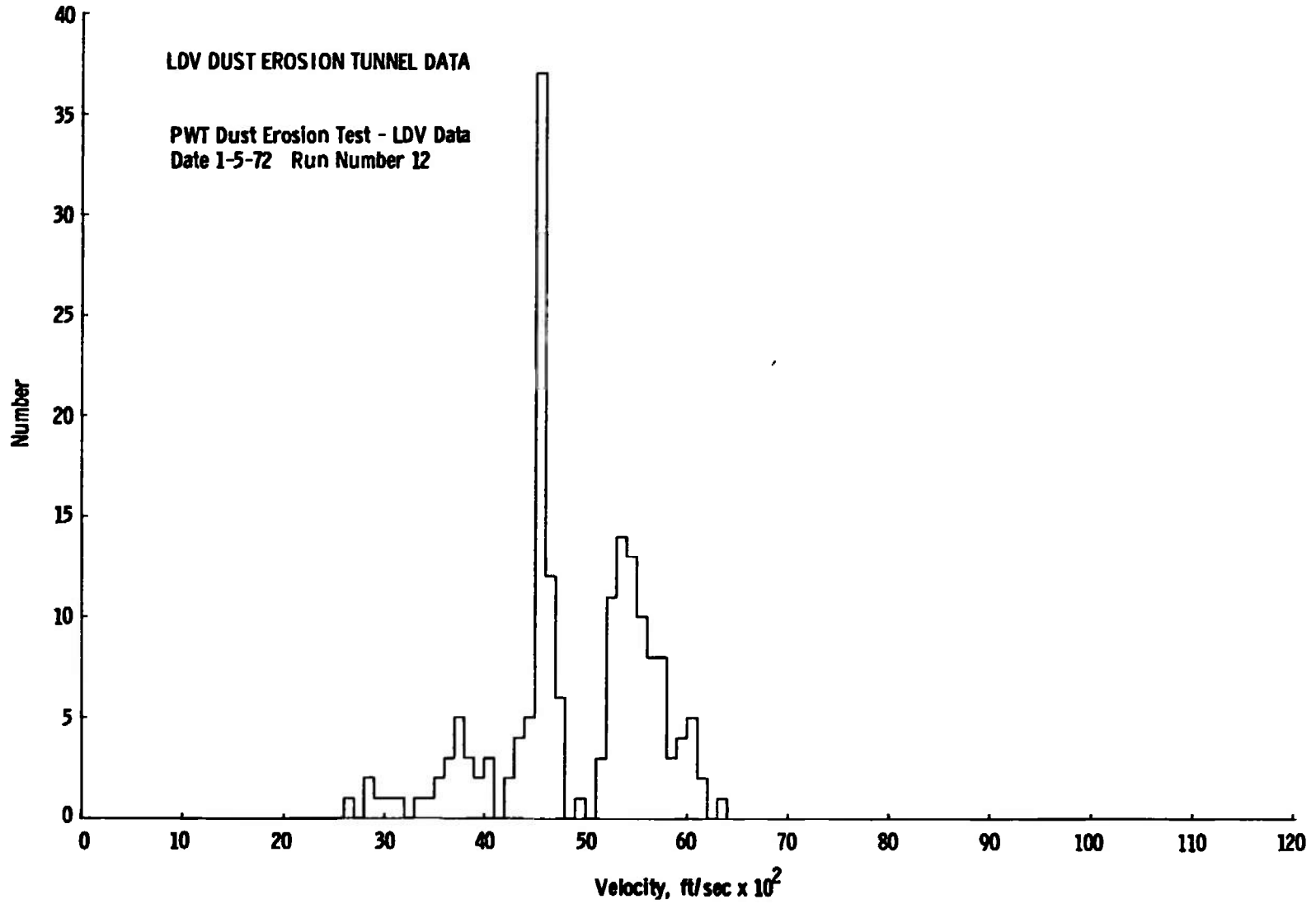


Fig. 18 Velocity Distribution - Run No. 12

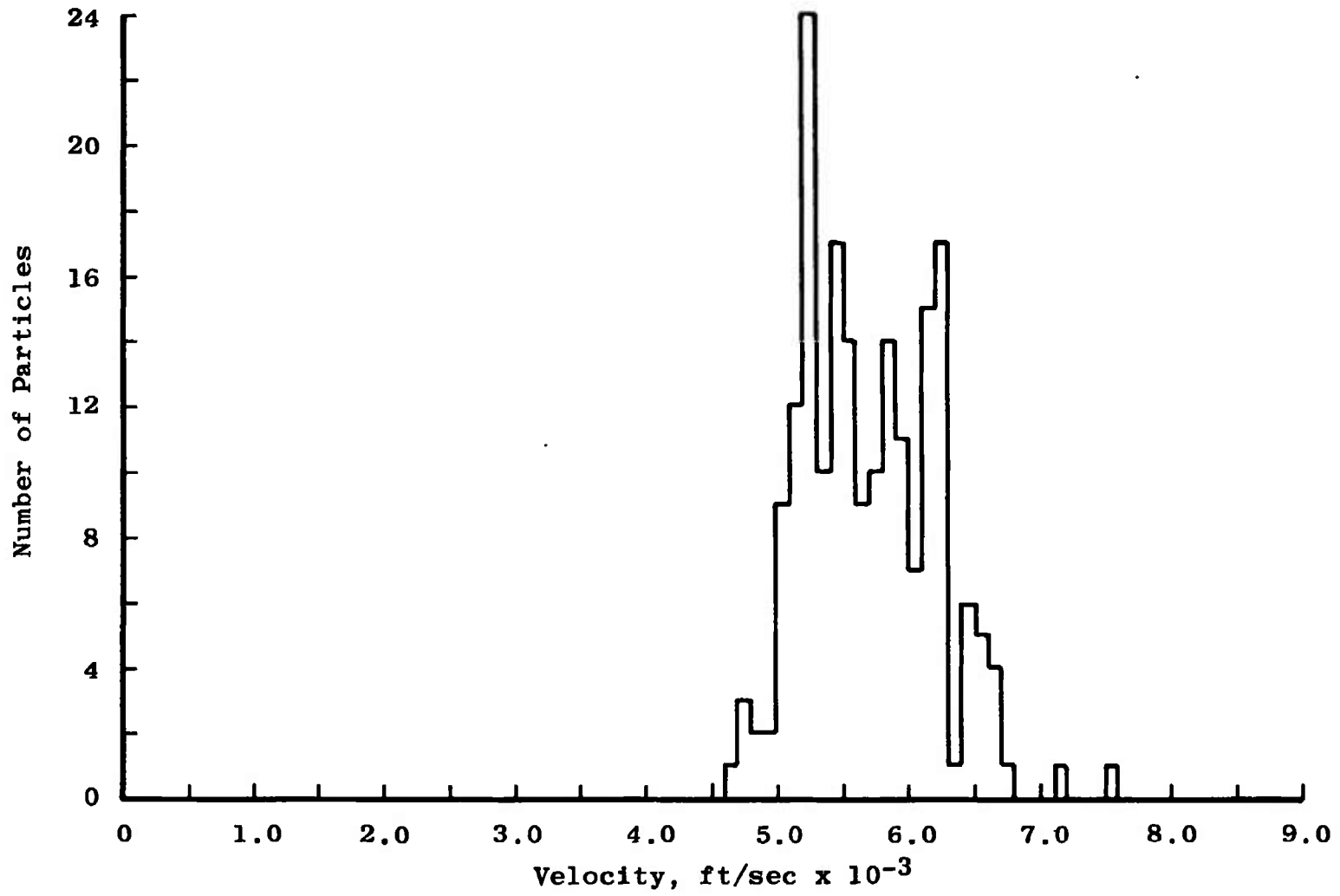


Fig. 19 Velocity Distribution Obtained by Holographic Technique – Run No. 1

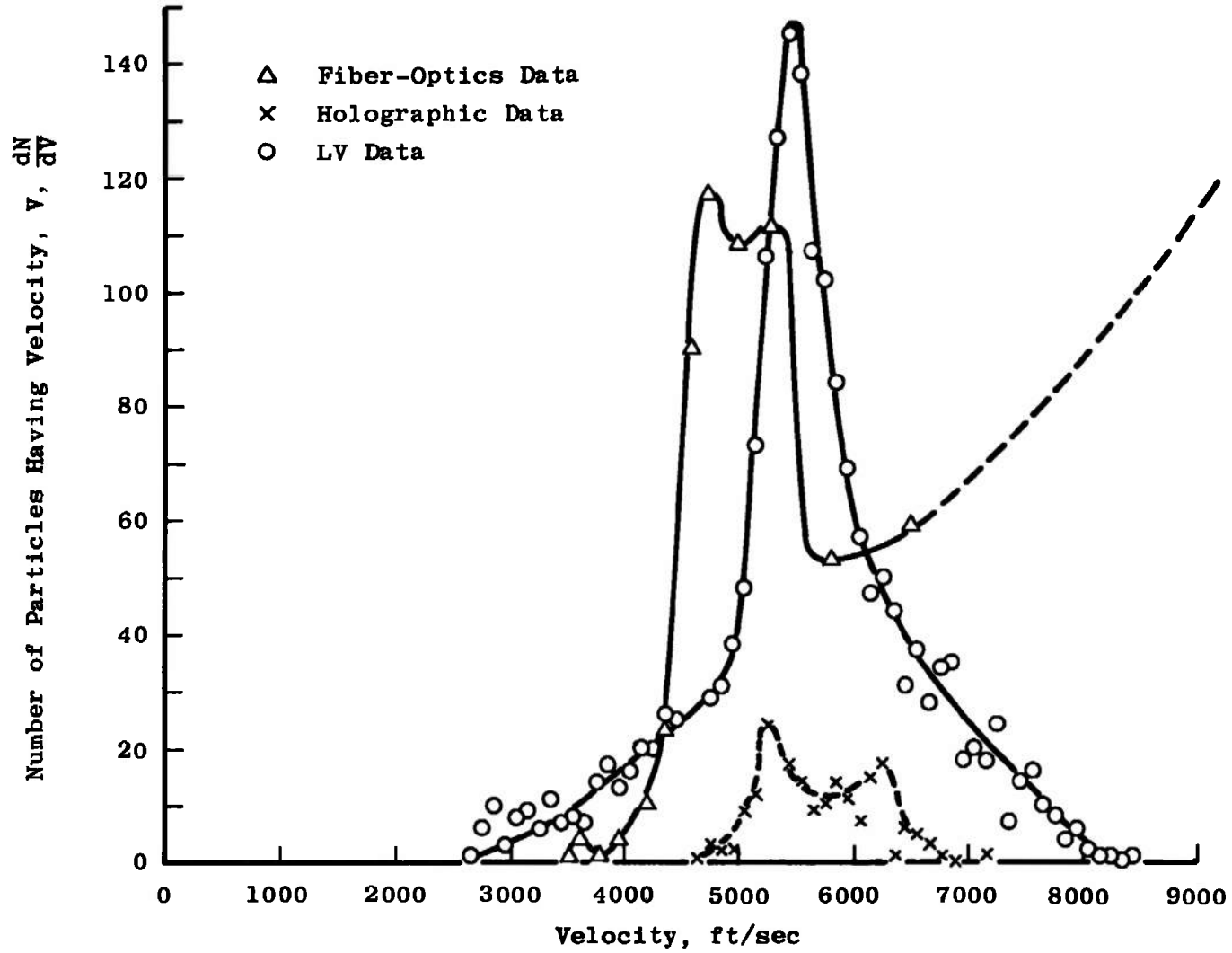
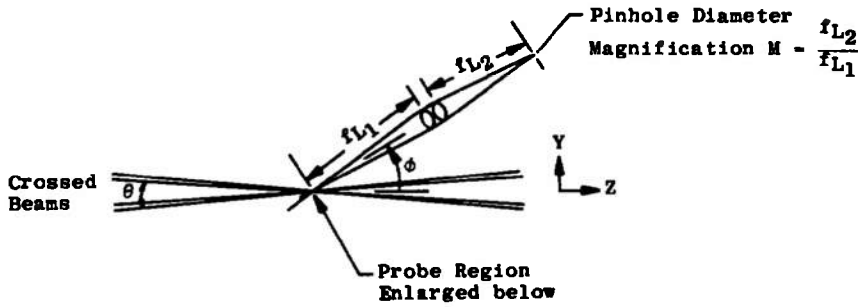


Fig. 20 Velocity Distribution Obtained by Three Experimental Techniques



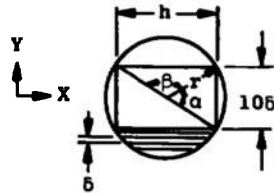
a. Typical Dual-Scatter LV System

Sensing Area Height:

$$h = 2 r \sin (\beta / 2)$$

$$\beta = 180 \text{ deg} - \alpha$$

$$\alpha = 2 \sin^{-1} (56 / r)$$



b. Probe Volume, End View

Sensing Area Width (avg):

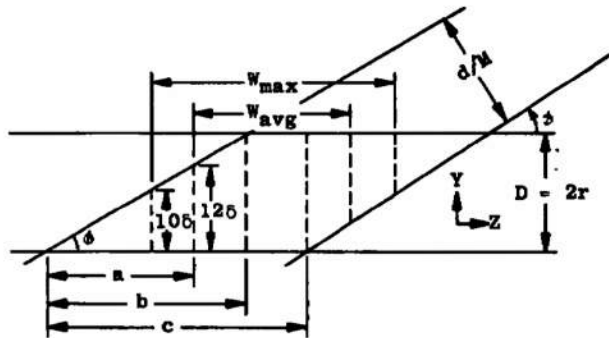
$$W_{avg} = 2(b - a) + (c - b)$$

where

$$a = \frac{126}{\tan \phi}$$

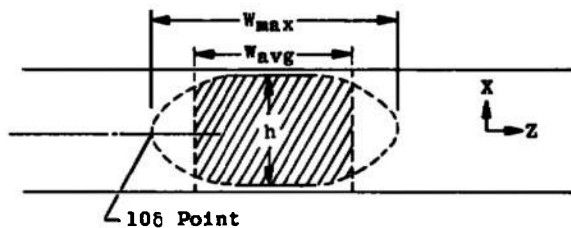
$$b = \frac{D}{\tan \beta}$$

$$c = \frac{d}{M \sin \phi}$$



c. Probe Volume, Plan View

$$\text{Area (avg)} = h \times W_{avg}$$



d. Probe Volume, Side View

Fig. 21 LV Probe Volume Illustration

UNCLASSIFIED

Security Classification

DOCUMENT CONTROL DATA - R & D

(Security classification of title, body of abstract and indexing annotation must be entered when the overall report is classified)

1. ORIGINATING ACTIVITY (Corporate author) Arnold Engineering Development Center Arnold Air Force Station, Tennessee 37389		2a. REPORT SECURITY CLASSIFICATION UNCLASSIFIED	
		2b. GROUP N/A	
3. REPORT TITLE DUST PARTICLE VELOCITY MEASUREMENTS USING A LASER VELOCIMETER			
4. DESCRIPTIVE NOTES (Type of report and inclusive dates) November 1971 through February 1972 - Final Report			
5. AUTHOR(S) (First name, middle initial, last name) V. A. Cline, Jr., ARO, Inc.			
6. REPORT DATE December 1972		7a. TOTAL NO. OF PAGES 37	7b. NO OF REFS 7
8a. CONTRACT OR GRANT NO		9a. ORIGINATOR'S REPORT NUMBER(S) AEDC-TR-72-159	
b. PROJECT NO		9b. OTHER REPORT NO(S) (Any other numbers that may be assigned this report) ARO-OMD-TR-72-136	
c. Program Element 65802F			
d.			
10. DISTRIBUTION STATEMENT Approved for public release; distribution unlimited.			
11. SUPPLEMENTARY NOTES Available in DDC.		12. SPONSORING MILITARY ACTIVITY Arnold Engineering Development Center, Air Force Systems Command, Arnold AF Station, Tennessee	
13. ABSTRACT This report describes the use of a one-component dual-scatter laser velocimeter (LV), in the forward-scatter mode, to measure the particle velocity distribution in a hypersonic dust erosion facility. The data acquired from a number of experiments are briefly summarized. Additional data acquired from holographic and fiber-optics measurements are also compared with the LV data. A discussion of the effects of both periodic and nonperiodic electrical noise upon the data is presented.			

KEY WORDS

LINK A

LINK B

LINK C

ROLE

WT

ROLE

WT

ROLE

WT

laser

velocimeter

dust

hypervelocity wind tunnel

hypervelocity impact

holography

fiber optics